Differentiating physical and biological storage of N along an intermittent Antarctic stream corridor

Joel G. Singley[1,2,3,6], Mark R. Salvatore[4,7], Michael N. Gooseff[2,5,8], Diane M. McKnight[2,5,9], and Eve-Lyn S. Hinckley[2,3,10]

[1]Biology, Marine Biology, and Environmental Science, Roger Williams University, 1 Old Ferry Road, Bristol, Rhode Island 02809 USA
[2]Institute of Arctic and Alpine Research, Campus Box 450, Boulder, Colorado 80309 USA
[3]Department of Environmental Studies, University of Colorado, MacAllister Building, 4001 Discovery Drive, Boulder, Colorado 80303 USA
[4]Department of Astronomy and Planetary Science, Northern Arizona University, 527 South Beaver Street, Flagstaff, Arizona 86011 USA
[5]Civil, Environmental, and Architectural Engineering, University of Colorado, 1111 Engineering Drive, Boulder, Colorado 80309 USA

Abstract: In many temperate streams, biological uptake of N acts to attenuate the transport of excess N from allochthonous anthropogenic imports. Relatively few studies have determined how this N uptake relates to the magnitude of physical vs biological N storage in the stream corridor, especially for intermittent systems where allochthonous N imports are often low and N transport may only occur during brief periods of streamflow. Glacial meltwater streams in the McMurdo Dry Valleys of Antarctica provide an excellent setting to quantify autochthonous N-cycling and storage processes supported by abundant algal mats and well-connected hyporheic zones. We combined historic point-scale sediment and periphyton sample datasets with remote sensing-based modeling of periphyton coverage to estimate how much N was stored in periphyton biomass and the hyporheic zone of a 5-km long McMurdo Dry Valley stream corridor (>100,000 m^2). We contextualized these N storage calculations by estimating the magnitude of annual N imports to and exports from the stream corridor based on >2 decades of streamflow and surface water data, source glacier ice cores and meltwater data, and past studies of local aeolian deposition and biological N fixation rates. We found that in this highly oligotrophic system, stream corridor-scale N storage was ~1000× that of total annual N import or export fluxes. More than 90% of this temporarily stored N was autochthonous organic matter in the shallow (<10 cm) hyporheic zone, which acts as a reservoir that sustains N availability in the water column. Despite its location in a polar desert devoid of higher-order vegetation, area-normalized N storage (~40 g N/m^2) was greater than that reported for streams at lower latitudes (~1–22 g N/m^2). We also demonstrated that NH_4^+ sorption to stream sediment may be an important physicochemical N storage mechanism that responds to short-term fluctuations in streamflow and governs the mobility of inorganic N. Altogether, this research illustrates the importance of quantifying N storage within stream corridors when evaluating the significance of internal cycling and physical retention processes that modulate N availability.

Key words: nutrient budget, nitrogen cycling, hyporheic zone, periphyton, organic matter, McMurdo LTER

Biogeochemical processes in small headwater streams regulate nutrient concentrations and exert a strong influence on nutrient fluxes to downstream ecosystems (Peterson et al. 2001, Alexander et al. 2007). Much of the research on biogeochemical cycling within streams has focused on nutrient retention, especially N sourced from the surrounding landscape (e.g., Boyer et al. 2002, Duncan et al. 2015, Drummond et al. 2016). Quantification of N retention in streams has centered on relationships between hydrologic connectivity and biogeochemical reaction rates (Gomez-Velez et al. 2015, Harvey et al. 2018) or a simple mass balance approach wherein retention is a residual term between import and output fluxes (Burns 1998, Seitzinger et al. 2006). Most studies have characterized reach-scale rates of N uptake based on removal of N added in excess of ambient conditions over very short durations. These flux- or transport-centric approaches

E-mail addresses: [6]jsingley@rwu.edu; [7]mark.salvatore@nau.edu; [8]michael.gooseff@colorado.edu; [9]diane.mcknight@colorado.edu; [10]eve.hinckley@colorado.edu

Received 1 October 2021; Accepted 6 October 2022; Published online 26 May 2023. Associate Editor, Sarah Roley.

  https://doi.org/10.1086/725676

have not sufficiently documented the extent of N storage within stream corridors, especially intermittent streams and oligotrophic environments with low allochthonous N imports.

In terrestrial biogeochemistry, the importance of particular N cycling processes is frequently contextualized by comparing the relative sizes of coupled pools and fluxes (Vitousek and Reiners 1975, Aber et al. 1989, 1998, Lovett and Goodale 2011), whereas only a few studies of stream corridors simultaneously quantify N storage pools and short-term uptake and release rates (Schmadel et al. 2021). This oversight has the potential to obscure important patterns in N cycling and storage among stream corridor systems. For example, a synthesis of 17 trace-level stable isotope N additions spanning the globe found that fine benthic organic matter (OM) accounted for the dominant fraction of N storage across all systems, whereas assimilatory uptake rates and the contribution from autotrophic and heterotrophic primary uptake compartments varied widely (Tank et al. 2018). Area-normalized storage among these systems ranged from 1 to 10 g/m^2.

A few other studies have also directly quantified N storage under ambient conditions without tracers. Such work demonstrated that in temperate forested systems, >90% of N storage was in the form of allochthonous detritus (Naiman and Melillo 1984, Triska et al. 1984). In contrast, Grimm (1987) found that >90% of N storage in a desert stream was in autochthonous detritus, although area-normalized N storage was lower than in forested systems (3–9 g/m^2 compared with 12–22 g/m^2). Altogether, these studies demonstrate that the form, magnitude, and temporal stability of N storage depends heavily on ecosystem characteristics, including OM sourcing, hydrologic variability, canopy cover, and net metabolic status.

Quantifying the storage of N across stream corridors is further complicated by the fact that N storage occurs through both biological and physical mechanisms (Naiman and Melillo 1984, Triska et al. 1984, Grimm 1987). In nutrient uptake experiments within the stream benthos, O'Brien et al. (2012) found that biotic assimilation of N into periphyton biomass was more important than denitrification for removing N. Most studies of N retention via biological uptake characterize spatial and temporal variations in small-scale area-normalized periphyton biomass (i.e., mg chlorophyll *a* [Chl *a*]/cm^2) in response to environmental conditions or nutrient availability (e.g., Horner and Welch 1981, Stelzer and Lamberti 2001, von Schiller et al. 2007, Koch et al. 2018). Focus on area-normalized biomass has ensured comparability of results at small scales among systems and allowed for cross-system synthesis (e.g., Dodds et al. 2002), but apart from the few whole-stream N-budget studies (e.g., Triska et al. 1984), biomass, or the N contained therein, is not scaled along entire reaches. Such scaling is hampered by the inherent patchiness of periphyton, often due to physical disturbance (i.e., scouring with flood pulses) or grazing processes (Hillebrand 2008, Luce et al. 2010). Yet, scaling N and algal biomass pools across an entire reach would permit benchmarking of stored N mass against total seasonal or annual N fluxes.

Apart from algal biomass in the stream, N can be transiently stored by physical processes in the hyporheic zone, such as by sorption to sediment (Triska et al. 1994), entrainment of particulate OM (POM) (Triska et al. 1984, Heindel et al. 2021a), and storage in dissolved form within interstitial waters (Grimm 1987, Bernhardt et al. 2005). As with total N storage, the relative magnitude and stability of these storage mechanisms at the reach scale is understudied but likely varies because of climate and flow regime. For example, it is known that NH_4^+ sorption can compete with biotic uptake (Triska et al. 1994) in temperate systems, but the conditions under which NH_4^+ sorption is reversible and the size of the adsorbed pool remain difficult to quantify in most streams. This knowledge gap is particularly relevant to intermittent streams that experience rapidly changing ionic concentrations and specific conductivities (Datry et al. 2017), which could theoretically alter cation exchange dynamics governing NH_4^+ sorption. The hyporheic zone can also entrain POM, which contains N. However, this mechanism for N storage is also transient because of mineralization and remobilization processes (Bernhardt et al. 2005, Burrows et al. 2017) that vary widely as a function of the climatic characteristics—especially temperature and annual precipitation—of intermittent stream systems (Shumilova et al. 2019). Lastly, N storage as dissolved solutes in the stream corridor, mainly in interstitial waters of hyporheic and riparian areas, is potentially even more transient because of relatively rapid turnover resulting from hydrologic exchange flows. In intermittent streams, much longer residence times result from diminished surface flow such that transient storage in the hyporheic zone may actually occur over longer timescales and with greater variations in space (Gómez et al. 2009). Therefore, the importance of particular N retention mechanisms may differ between perennial and intermittent streams.

Proglacial intermittent streams of the McMurdo Dry Valleys (MDVs) in Antarctica are often invoked as an ideal natural setting to investigate coupled physical and biological stream corridor processes (McKnight et al. 2015). Even in a cold and hyper-arid environment that is devoid of high-order plants and allochthonous OM imports, benthic algal mats cover extensive portions of streambeds (McKnight et al. 1998, 1999). These mats are dominated by cyanobacteria and are perennial, persisting in a freeze-dried state through the winter (McKnight et al. 1999). Along with heterotrophic microbes in the hyporheic and parafluvial zones, these mats contribute to biogeochemical cycling of N (Koch et al. 2010, Kohler et al. 2018, Singley et al. 2021b), including relatively rapid N removal from surface water (Gooseff et al. 2004b, McKnight et al. 2004) and N fixation (Howard-Williams et al. 1989, McKnight et al. 2007). The hyporheic zones of MDV streams contain elevated concentrations of dissolved

and adsorbed N (Heindel et al. 2021a, Singley et al. 2021b) and autochthonous OM in various states of decomposition (Heindel et al. 2021a). A prior study of the stable isotopic composition of mat biomass indicated that N fixed within the stream corridor supplants N imports from glacial meltwater as the primary N source with increasing distance downstream (Kohler et al. 2018). Despite these insights and their relative simplicity, N budgets for MDV streams remain poorly constrained, particularly the magnitude and mechanisms governing N storage relative to annual fluxes.

Our study objective was to improve understanding of N import, export, and storage dynamics in intermittent systems with low allochthonous inputs using the MDVs as an example. Specifically, we sought to better quantify stream corridor N storage and fluxes in this system by addressing 3 questions: 1) How large are annual N fluxes into and from an MDV stream corridor? 2) What are the quantities of N stored within stream corridor biomass and the hyporheic zone? and 3) Is NH_4^+ stored by sorption to sediment potentially released in response to short-term changes in conductivity?

METHODS

To address our research questions, we took advantage of multiple field, laboratory, and remote sensing techniques. We combined data from historic point-scale sampling of water, sediment, and biomass along with remote sensing analyses and uncertainty propagation to uniquely characterize N storage over an entire stream corridor and compare these results with other stream ecosystems. We also conducted a laboratory assay to assess the stability of NH_4^+ sorption as an N storage mechanism—which has been previously overlooked—in light of observed short-term changes in stream water conductivity. By synthesizing historic point-scale observations, remote sensing of algal mat abundance, and a laboratory assay, we differentiated the contributions of physical versus biological processes to N storage and annual fluxes and highlighted the importance of transient N storage in maintaining N availability at much larger scales than are typically considered.

We estimated N import and export fluxes and N storage for the Von Guerard Stream corridor by mining historic field and laboratory data from the McMurdo Long-Term Ecological Research project. We scaled site-specific data over areal and volumetric footprints representing the whole Von Guerard Stream corridor. Table 1 defines each parameter used in the calculations presented below and includes the references for publications or datasets from which values were obtained. We present variables and formulas below with generic dimensions (i.e., mass, length, or time) identified in square brackets. We have omitted unit conversions from the formulas for clarity in the text, but they are included in the accompanying code. For these calculations, we also used Monte Carlo simulations to propagate uncertainty from observational data. To do so, we fit distributions for each parameter to previously published datasets, for which individual sample data are available, with *fitdistrplus* (version 1.1-6; Delignette-Muller and Dutang 2015) in R (version 4.1.1; R Project for Statistical Computing, Vienna, Austria). The type of distribution that was fit to each dataset is noted in Table 1. When full datasets were not available, we drew parameter values from normal distributions described by summary statistics (i.e., mean and SD) reported in the literature. For each flux and N pool calculation, we randomly sampled 10,000 values for each variable and repeated the calculation based on these parameterizations. The R code and preformatted data files to reproduce all of these estimates, including the distribution fitting and sampling for Monte Carlo simulations as well as unit conversions, are publicly available on Zenodo (https://doi.org/10.5281/zenodo.6049121).

Study site

We focused our analysis on Von Guerard Stream, a 5-km long stream that runs north from its source glacier in the Kukri Hills to Lake Fryxell in Taylor Valley, Antarctica (Fig. 1). Von Guerard Stream has been gauged and sampled for both algal biomass and surface water chemistry by the McMurdo Long-Term Ecological Research project each austral summer since 1994. Channel morphology, streambed composition, and algal mat coverage vary along Von Guerard Stream (Alger 1997, Wlostowski et al. 2016), making it a useful model for the diversity of stream characteristics present in the MDVs. Streamflow in Von Guerard Stream occurs for just a few weeks to months each year (mean of 4.7 wk) and is characterized by large diel pulsing events and periods of intermittency (Wlostowski et al. 2016). The stream corridor is largely hydrologically disconnected from adjacent hillslopes because of the hyper-arid climate (Gooseff et al. 2016), with mean annual air temperature of –18°C (Doran et al. 2002) and mean annual precipitation of <100 mm water equivalent (Fountain et al. 2010). Continuous permafrost prevents groundwater exchange beyond the seasonally thawed active layer (Conovitz et al. 2006, Bockheim et al. 2007), thereby further constraining hydrologic connectivity (Gooseff et al. 2011). Although there is evidence of a deep groundwater system beneath the permafrost layer (Mikucki et al. 2015), there is currently no evidence that substantial exchange occurs between this system and Von Guerard Stream.

Despite these limitations on hydrologic connectivity in this system, N is imported into and exported out of the stream corridor by a variety of physical and biological processes. N imports to the stream corridor generally occur via meltwater mobilization of N deposited on glaciers and directly into the stream corridor (Witherow et al. 2006, Deuerling et al. 2014). Further N additions occur via in-channel N fixation by *Nostoc*-dominated black algal mats, which occur at the stream margins along with sparse mosses (Howard-Williams et al. 1989, McKnight et al. 2007, Kohler et al. 2018). Extensive *Phormidium*-dominated orange algal

Table 1. Literature-derived values used to estimate N fluxes and pools (Eqs 1–9). Parameters are listed in the order that they first appear in the manuscript. AFDM = ash-free dry mass, Chl *a* = chlorophyll *a*, DIN = dissolved inorganic N, DON = dissolved organic N, POM = particulate organic matter, PON = particulate organic N.

Symbol	Description	Value or distribution type[a]	Units	Sample count	Source[b]
Q_{total}	Total seasonal stream discharge	Varies by season	L	–	Gooseff and McKnight 2019
DIN_{gl}	DIN concentration in glacial ice and supraglacial meltwater	Gamma	µg N/L	875 ice	Bergstrom and Gooseff 2021a
				287 melt	Bergstrom and Gooseff 2021b
DIN_{sw}	DIN concentration in stream water from lower reaches	21.2 ± 22.5	µg N/L	74	Gooseff and Lyons 2022
DON_{gl}	DON concentration in glacial ice melt	92.5	µg N/L	2	Howard-Williams et al. 1989
DON_{sw}	DON concentration in stream water from lower reaches	34.0 ± 19.0	µg N/L	15	Singley et al. 2021b
PON_{gl}	PON concentration in glacial ice melt	0	mg N/L	2	Howard-Williams et al. 1989
POM_{sw}	POM concentration in stream water from lower reaches	Min = 1×10^{-4} Max = 2.59×10^{-2}	mg/L	35	Cullis et al. 2014
CN_{POM}	C:N of POM in stream water from lower reaches	9.51 ± 1.92	–	13	Kohler 2018
ω	N-fixation rate of *Nostoc* mats	8.11 ± 5.45	mg N m^{-2} d^{-1}	16	McKnight et al. 2007
D_{season}	Flow season duration	49.8 ± 15.3	d	22	Gooseff and McKnight 2019
A_{blk}	Total areal coverage by *Nostoc* mats	4000	m^2	–	McKnight et al. 1998
ϕ	Inorganic N deposition rate for Lake Fryxell	2.68	µg N m^{-2} y^{-1}	–	Deuerling et al. 2014
A_{VG}	Von Guerard Stream corridor area	134,112.5	m^2	–	
l_1	Upper reach length	1000	m	–	McKnight et al. 1998
l_2	Middle reach length	3500	m	–	McKnight et al. 1998
l_3	Lower reach length	500	m	–	McKnight et al. 1998
$w_{blk,1}$	*Nostoc* mat width in upper reach	0	m	–	McKnight et al. 1998
$w_{blk,2}$	*Nostoc* mat width in middle reach	1	m	–	McKnight et al. 1998
$w_{blk,3}$	*Nostoc* mat width in lower reach	1	m	–	McKnight et al. 1998
$w_{or,1}$	*Phormidium* mat width in upper reach	0.5	m	–	McKnight et al. 1998
$w_{or,2}$	*Phormidium* mat width in middle reach	3	m	–	McKnight et al. 1998
$w_{or,3}$	*Phormidium* mat width in lower reach	0.5	m	–	McKnight et al. 1998
$Chl_{blk,1}$	Chl *a* content of *Nostoc* mats in upper reach	0	µg Chl *a*/cm^2	–	McKnight et al. 1998
$Chl_{blk,2}$	Chl *a* content of *Nostoc* mats in middle reach	31	µg Chl *a*/cm^2	–	McKnight et al. 1998

Table 1. (*Continued*)

Symbol	Description	Value or distribution type[a]	Units	Sample count	Source[b]
$Chl_{blk,3}$	Chl *a* content of *Nostoc* mats in lower reach	9	μg Chl *a*/cm^2	–	McKnight et al. 1998
$Chl_{or,1}$	Chl *a* content of *Phormidium* mats in upper reach	4.7	μg Chl *a*/cm^2	–	McKnight et al. 1998
$Chl_{or,2}$	Chl *a* content of *Phormidium* mats in middle reach	12	μg Chl *a*/cm^2	–	McKnight et al. 1998
$Chl_{or,3}$	Chl *a* content of *Phormidium* mats in lower reach	31	μg Chl *a*/cm^2	–	McKnight et al. 1998
γ_{blk}	AFDM:Chl *a* of *Nostoc* mats	Gamma	mg AFDM/μg Chl *a*	130	McKnight 2019
γ_{or}	AFDM:Chl *a* of *Phormidium* mats	Gamma	mg AFDM/μg Chl *a*	141	McKnight 2019
CN_{blk}	C:N of *Nostoc* mats	9.1 ± 0.8	–	32	Kohler 2018
CN_{or}	C:N of *Phormidium* mats	10.5 ± 1.54	–	32	Kohler 2018
A_p	Pixel area from WorldView-3 imagery	1.95	m^2	–	–
τ_{blk}	Spatial coverage by *Nostoc* mats	Varies by pixel	%	–	–
τ_{or}	Spatial coverage by *Phormidium* mats	Varies by pixel	%	–	–
β_{blk}	Areal AFDM content of *Nostoc* mats	Gamma	AFDM/m^2	130	McKnight 2019
β_{or}	Areal AFDM content of *Phormidium* mats	Exponential	AFDM/m^2	141	McKnight 2019
l	Total stream length	5000	m	–	–
w_{hz}	Saturated hyporheic zone width	6	m	–	–
d	Hyporheic zone depth of seasonally thawed active layer	0.5	m		Conovitz et al. 2006
Φ	Hyporheic sediment porosity	0.34 ± 15.3	–	18	Heindel et al. 2021b
C_{nitr}	NO_3-N concentration of interstitial hyporheic water	78.6 ± 0.66	μg N/L	255	Singley et al. 2021b
w_{wet}	Wetted corridor width	9.54 ± 5.45	m	9	Heindel et al. 2021b
ρ	Hyporheic sediment bulk density	1749 ± 269.2	kg/m^3	18	Heindel et al. 2021b
C_{amm}	Adsorbed NH_4-N concentration for hyporheic sediment	0.679 ± 0.655	mg N/kg dry sediment	45	Heindel et al. 2021b
$d_{shallow}$	Shallow hyporheic depth based on sediment sample collection	0.1	m	–	Heindel et al. 2021b
LOI	Hyporheic organic matter content as AFDM	6.24 ± 1.34	g AFDM/kg dry sediment	45	Heindel et al. 2021b

[a] Values are provided where only a single value could be derived from the literature or where a normal distribution with the indicated mean ±SD were used. In all other instances the distribution type that was fitted to the raw data is identified.

[b] Values derived or assumed by this study do not have a source listed.

mats form broad cohesive films across many reaches but are not thought to be capable of N-fixation (McKnight et al. 2007, Kohler et al. 2018). Both black and orange algal mats are perennial, and even extreme high flows, such as occurred in January 2002 (Fig. S1), generally only decrease mat biomass by 2 to 3× (Cullis et al. 2014, Kohler et al. 2015). N can be exported as dissolved inorganic N (DIN), dissolved organic N (DON), and particulate organic N (PON) at the outlet into Lake Fryxell. Although denitrification has been observed in MDV streams during nutrient addition experiments

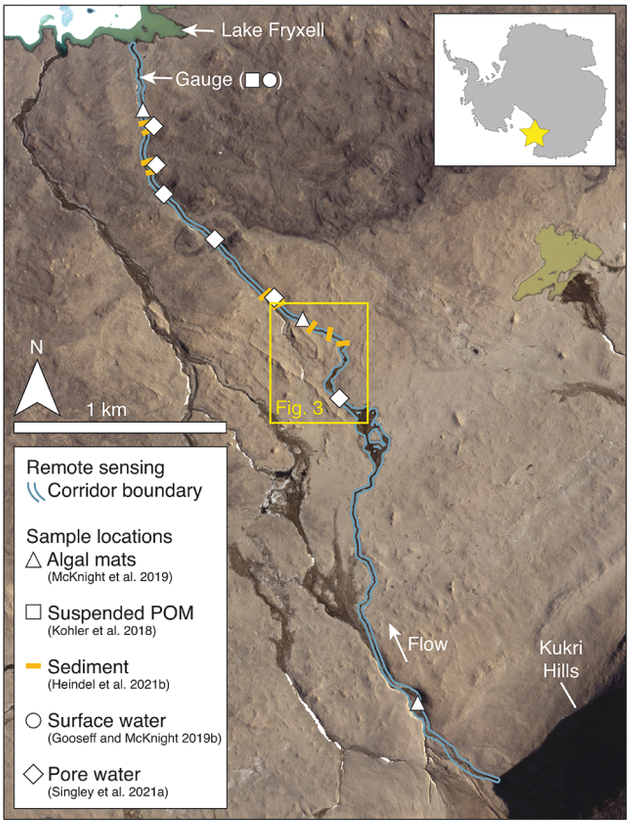

Figure 1. Von Guerard Stream in Taylor Valley, Antarctica (location marked with a star in the inset map), with stream corridor buffer (blue) used for remote sensing analysis and total area calculations. The image used for analysis covered the entire extent of this figure and the stream corridor. For reference, the extent of Fig. 3 is denoted by the yellow box. Historic sample locations from within the Von Guerard corridor are denoted, and samples from other locations (i.e., glacial ice, supraglacial meltwater, etc.) are available in the metadata for the referenced publications or datasets.

(Gooseff et al. 2004b), little is known about its contribution to N losses from the stream under ambient conditions.

Estimation of stream corridor N fluxes

We estimated seasonal dissolved and particulate N import and export fluxes based on 15-min discharge data (Gooseff and McKnight 2019) and concentration observations (1994–2019) from the gauge at the outlet of Von Guerard Stream into Lake Fryxell (Fig. 1). Because of highly dynamic and intermittent flow conditions (Fig. S1) as well as logistical constraints with polar fieldwork, stream water samples have historically been collected opportunistically (often once to twice weekly) during the streamflow season. For each season, we used the *pracma* package (version 2.3.3; Borchers 2021) in R to calculate total annual flow (Q_{total} [volume]) as the cumulative trapezoidal integration over the gap-filled discharge time series. We assumed no major gains or losses in discharge along the stream corridor such that we used the same Q_{total} values to calculate the fluxes at the head and outlet. For N imports, we used concentration data from MDV ice cores and supraglacial streams (Howard-Williams et al. 1989, Bergstrom and Gooseff 2021a, b), and we based export fluxes on observations of surface water in Von Guerard Stream (Singley et al. 2021a, Gooseff and Lyons 2022). The flux (F [mass]) for each dissolved and particulate constituent in a given flow season was calculated as:

$$F = CQ_{total}, \quad \text{(Eq. 1)}$$

where C is concentration [mass/length^3]. We repeated this calculation for each flow season (1995–2018) for both DIN and DON concentrations to ensure that the effects of highly variable seasonal discharge were reflected in our flux estimates. For imports from glacial sources, we calculated DIN concentrations as the sum of NH_4^+ and NO_3^- (combined analysis for $NO_3^- + NO_2^-$). Individual concentrations that were below the detection limits were treated as zeros in the DIN sum. For glacier ice, 58.6 and 18.7% of samples were below detection for NO_3^- and NH_4^+, respectively. For supraglacial stream water, 0.3 and 20.6% of samples were below detection for NO_3^- and NH_4^+, respectively. Detection limits varied within these datasets and over time, but all were $\leq$0.02 mg/L for NO_3^- and $\leq$0.005 mg/L for NH_4^+.

Similarly, we used DIN concentration data from historic grab samples collected in the lower reaches of Von Guerard Stream (1995–2018; Gooseff and Lyons 2022) to calculate export fluxes. For each grab sample, we calculated the DIN concentration as the sum of NO_3^-, NH_4^+, and NO_2^-. Individual concentrations that were below their respective detection limits (37.6 and 54.8% of all samples for NH_4^+ and NO_2^-, respectively) were again treated as zeros in the DIN sum. For the Monte Carlo simulations, we propagated uncertainty in these fluxes because of the variations in observed concentration data except for the DON import flux from the glacier, for which only a single value was available (Howard-Williams et al. 1989).

To our knowledge, only 1 prior study analyzed PON in MDV glacial ice melt, but no PON was detected (Howard-Williams et al. 1989). Consequently, we assume that the PON flux into Von Guerard Stream from its source glacier is negligible (~0 kg N/y). Along Von Guerard Stream, POM, which contains N, is mobilized in a hysteretic pattern from algal mats with each meltwater pulse (Cullis et al. 2014). Both POM concentrations and total fluxes differ among individual flood pulses as a function of the time since a resetting flood event and the regrowth of potentially mobile benthic biomass. Currently, there is insufficient information to adequately model these time-varying biomass pool dynamics and to generate continuous estimates of POM concentrations (C_{POM} [mass/length^3]), especially for multiple seasons. Thus, for tractability, we calculated the absolute boundaries of seasonal PON export fluxes (F_{PON} [mass]) as:

$$F_{\mathrm{PON}} = \frac{C_{\mathrm{POM}} Q_{\mathrm{total}}}{CN_{\mathrm{POM}}}. \quad \text{(Eq. 2)}$$

We used the observed C:N ratio of POM (CN_{POM} [mass:mass]) to obtain just the PON flux. For each season, we repeated this calculation with both the minimum and maximum C_{POM} observations reported by Cullis et al. (2014). The resulting estimates do not account for the complex interactions between biomass regrowth and POM mobilization but rather represent conservative estimates for the range of F_{PON}. We propagated uncertainty for CN_{POM} via the Monte Carlo simulations.

We calculated the annual biological N fixation flux (F_{fix} [mass]) for the stream corridor by scaling areal N fixation rates (ω [mass length^{-2} time^{-1}]) over the approximate black mat area (A_{blk} [length^2]; McKnight et al. 1998) and stream season flow duration (D_{season} [time]) as:

$$F_{\mathrm{fix}} = \omega A_{\mathrm{blk}} D_{\mathrm{season}}. \quad \text{(Eq. 3)}$$

We calculated D_{season} from 1995 to 2018 as the elapsed time in days between the 1$^{\mathrm{st}}$ and final gauged flows. We held the *Nostoc* area constant and used Monte Carlo simulations to propagate uncertainty for ω and D.

Lastly, we estimated total annual atmospheric deposition of inorganic N (F_{dep} [mass/time]) directly into the stream corridor. To do so, we scaled annual deposition rates estimated from Lake Fryxell (ϕ [mass length^{-2} time^{-1}]; Deuerling et al. 2014) over the entire Von Guerard Stream corridor (A_{VG} [length^2]).

$$F_{\mathrm{dep}} = \phi A_{\mathrm{VG}}. \quad \text{(Eq. 4)}$$

Estimation of stream corridor N pools

To quantify the relative importance of different storage mechanisms, we estimated total N in periphyton biomass, shallow (<10 cm) hyporheic OM, NH_4^+ adsorbed to hyporheic sediment, and dissolved NO_3^- in hyporheic water along the entire stream corridor. For all N pool estimates, we again propagated uncertainty by using Monte Carlo simulations based on fitting distributions to the field data or summary statistics. Individual parameter definitions and sources appear in Table 1.

N storage in periphyton biomass We estimated the total mass of N stored in benthic algal mat biomass in 2 different ways—1 that assumes spatially homogenous mat abundances and 1 that quantifies spatial heterogeneity. First, we estimated N in algal biomass (N_{bio} [mass]) in each mat type (black and orange) over 3 reaches (r) of various lengths (l_r [length]) and mat widths (w [length]) representing the entire length of Von Guerard Stream using a simple scaling calculation that does not account for spatial heterogeneity based on McKnight et al. (1998) as:

$$N_{\mathrm{bio}} = \sum_{r=1}^{3} \left(\frac{l_r w_{\mathrm{blk},r} chl_{\mathrm{blk},r} \gamma_{\mathrm{blk}}}{CN_{\mathrm{blk}}} + \frac{l_r w_{\mathrm{or},r} chl_{\mathrm{or},r} \gamma_{\mathrm{or}}}{CN_{\mathrm{or}}} \right), \quad \text{(Eq. 5)}$$

where $chl_{\mathrm{blk},r}$ and $chl_{\mathrm{or},r}$ are type- and reach-specific Chl *a* content [mass/length^2], $\gamma_{\mathrm{blk},r}$ and $\gamma_{\mathrm{or},r}$ are type- and reach-specific ash-free dry mass (AFDM) to chlorophyll ratios [mass:mass], and CN_{blk} and CN_{or} are C:N ratios [mass:mass] for each mat type. Here, we propagated uncertainty for each *chl*, γ, and *CN* parameter.

We also estimated spatial coverage of algal mats and N content based on analysis of multispectral satellite imagery and an MDV-specific spectral unmixing model (Salvatore et al. 2020), which allowed us to account for spatial heterogeneity of biomass that is not included in the simple scaling method described above. We based our analysis on data from a WorldView-3 (DigitalGlobe, now Maxar Technologies, Westminster, Colorado) image acquired on 26 January 2019 (catalog ID: 10400100485D6900). This image was acquired toward the end of the austral summer at a time with relatively little snow cover across most of the landscape and no streamflow for the entire 24 h preceding acquisition. Given the perennial nature of these mats, a single image toward the end of the summer is expected to be representative for typical flow seasons. As per Salvatore et al. (2020), we leveraged the unique spectral reflectance signatures of black and orange algal mats, moss, bare soil, and water to model the relative areal abundance of these surface endmembers in each pixel of a multispectral satellite image. We used a nonnegative spectral unmixing model that linearly combines a suite of endmember spectra to produce the best mathematical fit between the input spectrum and the model output. Salvatore et al. (2020) demonstrated that surface endmembers from the vicinity of Lake Fryxell are optically opaque and, therefore, can be appropriately modeled as a linear combination of their areal abundances (Salvatore et al. 2020). The root-mean-square error (RMSE) represents the goodness of fit between the observed and modeled spectra. We calculated RMSE for every modeled pixel, averaging 1.6% with an SD of 2.4% and a median of 1.2%. Less than 0.5% of all modeled pixels exhibited an RMSE of >10%.

From the individual mat coverage estimates by type and pixel, we then calculated N content of all algal biomass ($N_{\mathrm{bio}*}$) in the stream corridor as:

$$N_{\mathrm{bio}*} = \sum_{i}^{n_p} \left(\frac{\tau_{\mathrm{blk},i} \beta_{\mathrm{blk},i} A_p}{CN_{\mathrm{blk}}} \right) + \left(\frac{\tau_{\mathrm{or},i} \beta_{\mathrm{or},i} A_p}{CN_{\mathrm{or}}} \right). \quad \text{(Eq. 6)}$$

Here, we sum the N content of each mat type for each pixel (i) across the 68,767 pixels (n_{p}) within a 134,100-m^2 region that encompasses an ~10-m wide buffer to either side of the thalweg of Von Guerard Stream (Fig. 1). This width is approximately double the distance between the visible wetted margins for Von Guerard Stream reported by Heindel et al. (2021b) at low flows (<0.5 L/s). We converted % coverage (τ) for each pixel by mat type to AFDM based on areal

biomass (β [mass/length^2]) from field samples for Von Guerard Stream and average pixel area (A_p [length^2]). Lastly, we used the same C:N ratios noted above to convert AFDM to N content. In this estimation, we propagated uncertainty for β and CN by mat type.

N storage in the hyporheic zone Following Singley et al. (2021b), we estimated the mean N pool contained in dissolved NO_3^- in interstitial hyporheic waters of Von Guerard Stream from an extensive set of samples ($n = 255$; Singley et al. 2021a) as:

$$N_{nitr} = lw_{hz}d\Phi C_{nitr}. \quad \text{(Eq. 7)}$$

Here, we scaled dissolved NO_3^- concentrations (C_{nitr} [mass/length^3]) over the entire pore space within a volume defined by the saturated sediment width (w_{hz} [length]), stream length (l [length]), active layer depth (d [length]), and hyporheic sediment porosity (Φ [-]). We limited this analysis to NO_3^- (as $NO_3^- + NO_2^-$) because NH_4^+ concentrations were often much lower than NO_3^- (Singley et al. 2021b) or below detection (64.9% of 255 samples; Singley et al. 2021a). We used normal distributions fitted to each dataset for uncertainty propagation for Φ and C_{nitr}.

Hyporheic sediments of Von Guerard Stream also contain OM (both heterotrophic bacteria and POM from algal mats) as well as NH_4^+ adsorbed to sediment (Heindel et al. 2021a). We scaled up mean hyporheic OM content from measured loss on ignition (*LOI*; AFDM/g dry soil) and sediment mass-normalized concentration of NH_4^+ (C_{amm} [mass:mass]) across the estimated mass of sediment in their respective volumes based on observed sediment bulk density (ρ [mass/length^3]). We calculated the total N mass in each of these pools as:

$$N_{adsorbed} = lw_{wet}d\rho C_{amm}, \quad \text{(Eq. 8)}$$

$$N_{hyp,OM} = \frac{lw_{wet}d_{shallow}\rho LOI}{CN_{blk}}. \quad \text{(Eq. 9)}$$

For $N_{adsorbed}$ we set d to 0.5 m, just as for the dissolved NO_3^- pool calculation. For $N_{hyp,om}$ we limited the analysis to a shallow depth ($d_{shallow}$) of only 0.1 m, given the sample collection protocol used by Heindel et al. (2021b). Because most POM entrained in the hyporheic zone can be traced to black mats (Heindel et al. 2021a), we used the CN_{blk} data to convert AFDM to N in the $N_{hyp,OM}$ calculation. For these estimations, we propagated uncertainty in the Monte Carlo simulations by fitting and drawing values from normal distributions based on the data for w_{wet}, ρ, C_{amm}, *LOI*, and CN_{blk}.

Assay on desorption of NH_4^+ from stream sediment

We performed a laboratory assay on sediment samples collected from the lower reaches of Von Guerard Stream (Fig. 1) to assess the availability of NH_4^+ adsorbed to stream sediment as a potential source for internal DIN fluxes due to variations in stream water chemistry. Specifically, we conducted an assay to determine whether NH_4^+ desorbed over the range of conductivities observed in Von Guerard Stream from 1995 to 2015 (Fig. 2A).

We collected sediment samples from the top 10 cm of the streambed at 5 locations along a transect spanning between the wetted margins of the stream corridor. Subsamples from this sediment were previously analyzed for OM content through *LOI* in a muffle furnace and total extractable NH_4^+ by 2M KCl extraction. A full description of sediment sample collection, storage, and analytical methods is provided by Heindel et al. (2021a, b). For this study, we thawed sediment samples at 4°C and weighed 15 subsamples (~20 g of sediment each) for 5 lateral locations from the P2 transect (total subsample $n = 75$; see Heindel et al. 2021b) into 250-mL high density polyethylene bottles. We prepared treatment solutions containing KCl and deionized water to achieve specific conductivity (SC) values that reflect the range of diel to seasonal fluctuations of SC observed in Von Guerard Stream (Fig. 2B). Based on measurements with a temperature-corrected benchtop conductivity probe, the treatment solution SC values were 0.06 (deionized water only), 40.7, 77.1, 155.9, and 317.7 µS/cm.

For this assay, we exposed sediment to each of the treatment solutions to observe changes in ion concentrations due to reversible adsorption. In particular, we mixed 3 of the subsamples from each of the 5 locations with each treatment solution at a 2:5 ratio of sediment to solution by mass. We immediately placed the resulting sediment slurries ($n = 15$) and solution blank for each treatment on a rotary shaker table at 300 rpm for 1 h, then centrifuged them at 3000 rpm for 5 min and filtered them via GF/F filters (Whatman, Maidstone, United Kingdom). We stored the filtrate frozen (–20°C) until analysis. We analyzed NH_4^+ concentrations with a Lachat Quickchem Flow Injection Analysis System (Hach®, Loveland, Colorado) according to standard protocol 4500-NH3 H (phenolate flow injection analysis; SMC APHA 2018a), with a minimum detection limit of 5 µg NH_4-N/L. We analyzed NO_3^- as the sum of NO_3^- and NO_2^- by standard method 4500-NO_3 I (cadmium reduction flow injection; SMC APHA 2018b) with a detection limit of 4 µg NO_3–N/L. We calculated sample-specific sediment dry masses based on gravimetric moisture content for each transect reported by Heindel et al. (2021a). We then normalized the filtrate N concentrations to sediment dry mass for each sample to enable comparisons. We measured incubation solution concentrations of K^+ and Cl^- by atomic absorption spectrophotometry with detection limits of 4 and 30 µg/L, respectively.

We visualized these data to qualitatively examine relationships between solution SC and the net mass of DIN released/mass dry sediment and the percentage of total extractable NH_4^+ for each site. We also compared changes in concentrations of K^+ and Cl^- to determine whether cation exchange was a likely explanation for any observed release of NH_4^+. We did not complete correlation or regression

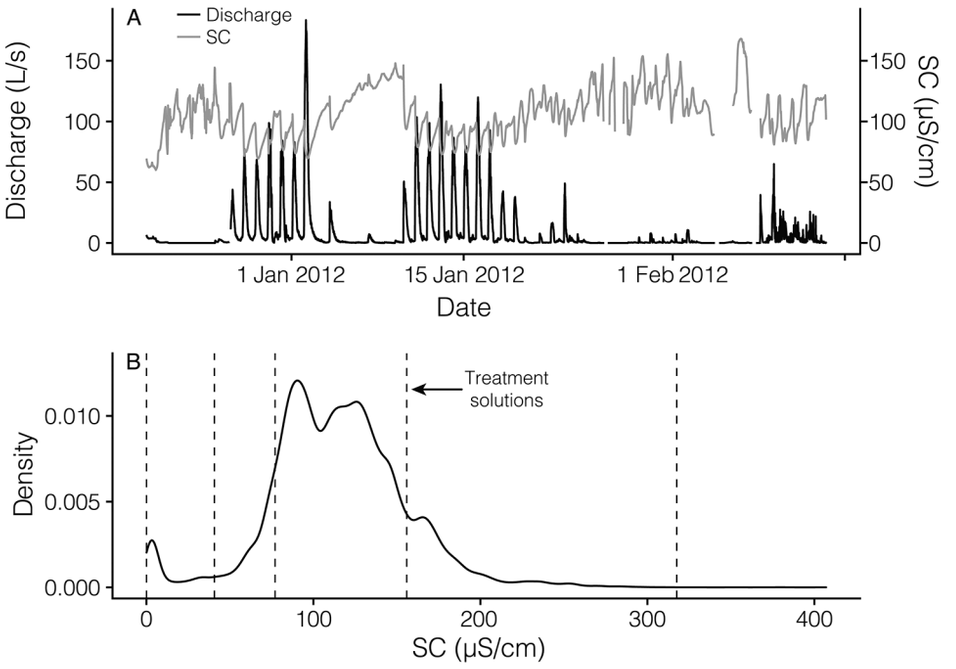

Figure 2. Illustrative discharge and specific conductivity (SC) variability from the 2012 flow season in Von Guerard Stream, Antarctica (A). Historic (1995–2015) SC distribution for high-frequency surface water observations with laboratory assay treatment solution values shown as dashed vertical lines (B).

analysis because of several constraints associated with conducting this assay on sediment from this study system. Specifically, we did not utilize a kill treatment to limit biological activity because preliminary trials found that 1% formalin solutions may have substantially altered cation exchange through changes to solution pH. Similarly, buffered formalin contains ion concentrations that exceeded the low conductivities needed to replicate MDV stream water observations, so a formalin kill was not suitable for this assay. We also did not autoclave sediment because a prior study reported potential releases of N and P during such treatment of MDV sediments (Bergstrom et al. 2020). Consequently, the results from this assay reflect only the potential for NH_4^+ to desorb from stream sediment in response to changing stream water conductivities, not in situ dynamics or kinetics.

RESULTS

Seasonal N fluxes to and from the Von Guerard Stream corridor

We calculated annual fluxes of N to and from Von Guerard Stream while accounting for both variation in total annual streamflow and the distribution of N concentrations observed in glacial ice, supraglacial meltwater, and streamflow. Here we report the median followed by the interquartile range (1^{st}–3^{rd} quartiles) in parentheses. We do not report means or the SD because multiple pool estimates have highly skewed non-normal distributions resulting from the underlying distributions of field measurements. The code published on Zenodo (mentioned in Methods) to reproduce our analysis does provide these values.

On an annual basis, the import fluxes from the source glacier meltwater totaled 4.0 kg N/y (1.3–13.7). This total flux was composed of 1.1 kg N/y (0.3–4.3) as DIN, 2.9 kg N/y (0.9–9.3) as DON, and negligible PON imports. We estimated that N fixation by *Nostoc* in the stream corridor adds a further 1.5 kg N/y (0.8–2.4), and direct atmospheric deposition of inorganic N is very small (<<0.01 kg N/y). Combined, these fluxes amount to total imports of 5.4 kg N/y (2.0–16.0), which, normalized over the entire stream corridor, is equivalent to a gross import of 40.8 mg N m^{-2} y^{-1} (15.0–119.5). We again emphasize that because of limited hydrologic connectivity of MDV streams, these imports occur only through glacial meltwater inflows at the stream head, aerial deposition, and biological N fixation, not lateral or groundwater inflows along the stream.

We estimated that 1.2 kg N/y (0.3–5.5) is exported from the stream corridor in particulate and dissolved form annually. Specifically, we estimated that N fluxes as DIN from Von Guerard Stream into Lake Fryxell totaled 0.3 kg N/y (0.1–1.8). DON export was slightly larger at 0.8 kg N/y (0.2–3.4). Based on maximum observed concentrations across all flow conditions, N export as PON was ≤0.1 kg N/y (0.02–0.3). Notably, cumulative annual streamflow volume varied widely (719.5–2.76 × 10^8 L) and with no identified directional relationship between DIN or DON concentrations and

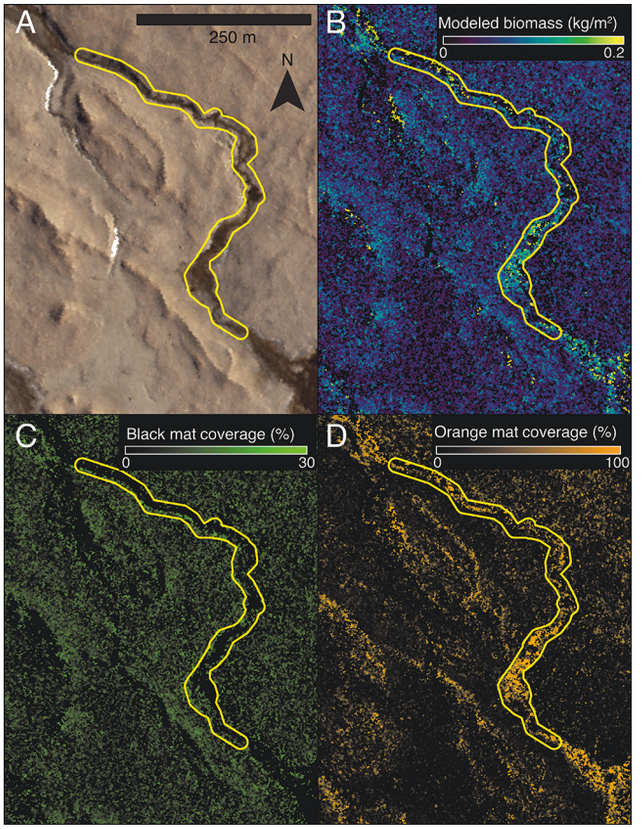

Figure 3. Modeled biomass and mat coverage from multispectral remote sensing data along reach 6 of the Von Guerard Stream corridor. Visible spectrum with corridor buffer ~10 m to either side of the thalweg; flow is from bottom to top (A). Modeled biomass (B), % coverage by *Nostoc*-dominated black mats (C), and % coverage by *Phormidium*-dominated orange mats (D) from linear unmixing model applied to multispectral data. Scale and orientation are the same for all panels.

discharge (i.e., diluting or enriching). N flux estimates into Lake Fryxell are primarily governed by variations in Q_{total} from 1 season to the next. We estimated that only ~17% of N imports are likely exported from the Von Guerard Stream corridor on an annual basis, although we could not account for losses via denitrification. Scaled to stream corridor area, exports amount to a gross N release of 9.1 mg N m^{-2} y^{-1} (2.4–41.0), resulting in a probable net accumulation in storage of 31.7 mg N m^{-2} y^{-1} (0.8–78.5). Although the ranges in magnitude of possible imports and exports do overlap, suggesting that there may be seasonally distinct shifts in the net direction of N storage, a tendency toward net accumulation in most years would be consistent with generating the large N storage pools we observed.

Estimates of periphyton biomass coverage by remote sensing

Estimates of algal biomass and N stored therein were remarkably comparable between simplified conceptual estimates (sensu McKnight et al. 1998) and those based on spectral analysis of satellite imagery (27% difference on the medians). Specifically, median (quartiles 1–3) N storage in biomass based on the simplified conceptual estimate (sensu McKnight et al. 1998) was 196.6 kg N (86.4–389.1), whereas our remote sensing method estimated biomass storage of 270.7 kg N (162.5–448.1). Generally, modeled algal mat abundances showed the greatest biomass in the stream channel, especially for orange mats (Fig. 3A–D). Patchy black mats are known to occur throughout the landscape, especially where snow patches form each winter. However, the modeled presence of orange mats outside the channel was unexpected. This predicted orange mat occurrence was most likely due to the presence of chlorophyll-bearing photosynthetic species present at small abundances throughout the landscape, either as mosses or disaggregated mat communities, that contribute to weakly photosynthetic signatures in the surrounding soils (Adams et al. 2006, Salvatore et al. 2020). The high abundance of orange mats within the stream corridor, in addition to the dominance of black mats along the stream margins, matches in situ observations (Alger 1997, McKnight et al. 1998, 1999) and previously published remote-sensing results (Salvatore et al. 2020). Finally, although we only analyzed a single image from late in 1 season, these estimates may be representative for end of summer conditions for summers with typical flow regimes. This snapshot does not reflect the cycles of growth, scouring, and regrowth that can occur throughout each austral summer or variations between years.

Stream corridor-scale N storage

We found that relative to the seasonal N import and export fluxes, large masses of N were physically and biologically stored along the stream corridor (Fig. 4A–C). In addition to the estimates of N stored in biomass reported above, we found that most Monte Carlo simulations (>70%) resulted in estimates wherein >90% of the total N stored in the stream corridor was found in the hyporheic zone as OM dissolved in porewater and as NH_4^+ adsorbed to sediment. OM in just the top 10 cm of sediment may account for ~4700 kg N (3600–6100). Additionally, we estimated that the hyporheic zone likely stored on the order of 30.6 kg N (16.5–49.4) in adsorbed NH_4^+ and 0.4 kg N (0.3–0.5) in dissolved NO_3^-. Combining the median estimate for each N pool and normalizing over the largest pool area (134,112.5 m^2), we obtained a total N storage estimate of ~40 g/m^2.

It is important to note that total N storage exceeded the mean annual flux of N at the outlet of Von Guerard Stream (Fig. 4A–C). The only exception was for N stored in dissolved NO_3^- in hyporheic waters, which was expected to be more transiently mobile and was of comparable size to, or slightly less than, seasonal N fluxes. In total, median annual imports and exports were <0.5 and <0.1% of median N storage in all pools, respectively.

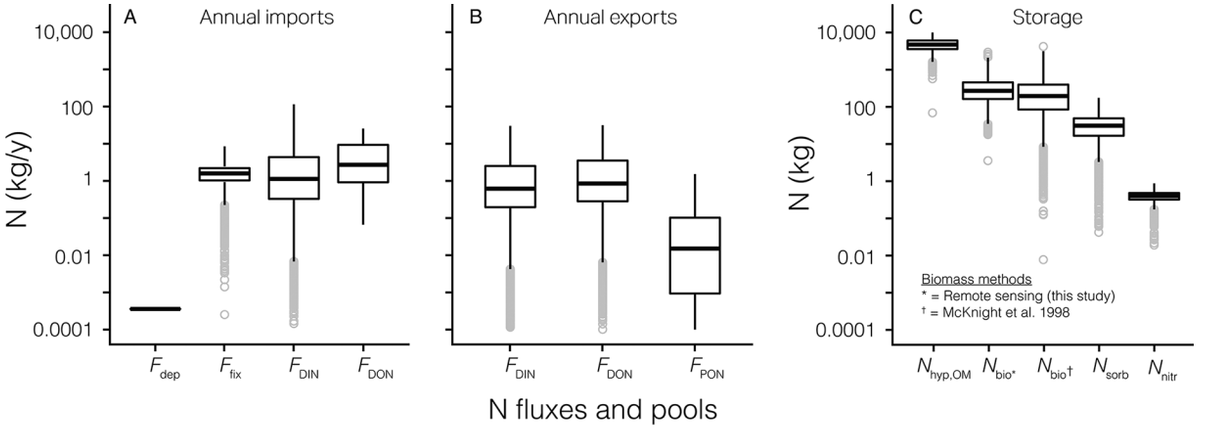

Figure 4. Estimates of annual N import fluxes (A), annual N export fluxes (B), and N storage pool sizes (C) with uncertainty propagation through Monte Carlo simulations (n = 10,000). The lower and upper box boundaries correspond to the 1st and 3rd quartiles, and the inner horizontal line is the median. Whiskers extend to 1.5× the interquartile range above and below the 1st and 3rd quartiles. Data beyond these ranges are denoted with light gray circles. Vertical axes are scaled logarithmically to aid comparison across multiple orders of magnitude. Annual N fluxes are abbreviated as F_{dep} for atmospheric deposition, F_{fix} for biological fixation, and F_{DIN}, F_{DON}, and F_{PON} for dissolved inorganic N, dissolved organic N, and particulate organic N in surface water, respectively. N storage pools are abbreviated as $N_{hyp,OM}$ for hyporheic organic matter, N_{bio*} for remotely sensed models of algal biomass, N_{bio}† for simple scaling estimates of algal biomass (McKnight et al. 1998 method), N_{sorb} for NH_4-N adsorbed to stream sediment, and N_{nitr} for dissolved NO_3-N in the hyporheic zone.

NH_4^+ desorption in response to changing SC

Our laboratory assay on stream sediment demonstrated that more K^+ than Cl^- was lost from solution with increasing SC (Fig. 5A). For the 2 lowest concentration treatments, K^+ and Cl^- concentrations increased slightly, suggesting that some additional ions were mobilized from the sediment as they were wetted. Losses of K^+ in the 77.1, 155.9, and 317.6 µS/cm treatments were not matched by similar losses of Cl^- despite comparable ionic masses. This result suggests that greater net cation, but not anion, exchange was occurring. This pattern is consistent with field observations of ion exchange during a previous tracer study in an MDV stream (Gooseff et al. 2004a).

We also found that NH_4^+ adsorbed to Von Guerard Stream sediments can be rapidly liberated into solution as SC increases (Fig. 5B, C). We also found that apparent differences in the net mass of NH_4^+ released, expressed as µg/g dry mass, were reflective of differences in the amount of total extractable NH_4^+. In other words, although the concentration of NH_4^+ stored by sorption varies laterally across the stream (Heindel et al. 2021a), similar proportions of total stored NH_4^+ are released for particular SC values (Fig. 5B). We also observed a potential trend towards plateauing of K^+ losses at higher concentrations (Fig. 5A), which may indicate an upper limit to cation exchange and, potentially, NH_4^+ desorption (i.e., neither 100% of K^+ was lost or NH_4^+ released) under reasonably representative SC values for Von Guerard Stream.

DISCUSSION

In this study, we leveraged historic point-scale sampling, remote-sensing analysis, and a laboratory assay to demonstrate that N storage is surprisingly high compared with observed fluxes in an intermittent Antarctic stream corridor. We uniquely scaled biological and physical N storage over the entire stream corridor (>100,000 m^2) to contextualize the importance of N storage at the ecosystem rather than centimeter scale. We found that even without significant allochthonous N imports, N storage, especially in the hyporheic zone, can be comparable—or potentially higher—than has been reported for lower latitude and even temperate forested systems. We also demonstrated that, despite generally being ignored outside of tracer addition studies, NH_4^+ adsorption to stream sediment may be an important transient physicochemical storage mechanism that responds to short-term fluctuations in streamflow and governs the mobility of inorganic N. Altogether, this work illustrates the necessity of quantifying N storage within stream corridors to determine the importance of autochthonous production, internal cycling, and retention in modulating and sustaining the availability of N.

High stream corridor storage of N relative to fluxes

We found that, despite the uncertainty in field data and scaling values over large areas (>100,000 m^2), there is substantially more N stored in biomass and the hyporheic zone than is exported from the stream corridor in any given flow season (Fig. 4C). We estimated that mean annual import and export of N represents <0.5% of the N that is physically and biologically stored within the stream corridor. Our results demonstrate that relatively substantial N storage in the stream corridor can occur even without allochthonous POM imports, which dominate stream corridor N storage

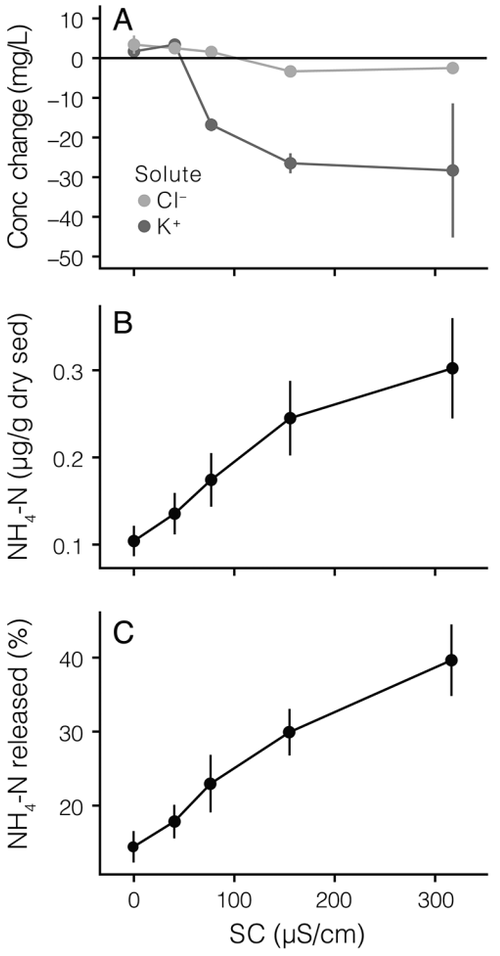

Figure 5. Changes in incubation solution ion concentrations (Conc) and responses of sediment (sed) adsorbed NH_4–N to increasing specific conductivity (SC). Changes in solution Conc of Cl^- and K^+ (mean ±SE) by treatment conductivity ($n = 5$) (A), assay treatment solution SC against mean (±SE) net mass of desorbed NH_4-N normalized to dry sed mass ($n = 15$) (B), and mean (±SE) net % of total extractable NH_4-N desorbed ($n = 15$) (C).

in forested temperate catchments (Naiman and Melillo 1984, Triska et al. 1984). At about 40 g/m^2, the area-normalized N storage we estimated for Von Guerard Stream was larger than the 12 to 22 g/m^2 estimated for headwater streams in temperate forests or the 3 to 9 g/m^2 for a mid-latitude desert stream (Naiman and Melillo 1984, Triska et al. 1984, Grimm 1987; Table 2). Our N storage estimate for Von Guerard Stream is also larger than the range of 1 to 10 g/m^2 reported for 17 streams spanning a wide range of systems (Tank et al. 2018; Table 2). Notably, this latter study did not quantify or include adsorbed NH_4^+, DIN in interstitial waters, or the sampling from parafluvial zones that were not actively inundated by flow at the time of the study, as we did here. The extreme hydrologic variability in MDV streams necessitates inclusion of these broad parafluvial zones, which somewhat complicates exact comparisons with these other systems where the lateral extent of streamflow does not vary so frequently on sub-hourly timescales.

Although we expected algal biomass to store the largest mass of N in MDV streams, given extensive benthic algal mat coverage (Alger 1997), absence of canopy cover, and lack of allochthonous litter imports, we found that most (>90%) stored N is likely held in the hyporheic zone. This pattern is consistent with the universal fractional dominance of N storage in fine benthic OM reported across climatic regions from –45°S to 67°N by Tank et al. (2018).

It is possible that our mean estimates of N storage in Von Guerard Stream are not entirely accurate because of our use of results from point-scale samples in the calculations. It is notable that even an order of magnitude reduction in total N mass stored would result in area-normalized storage that is comparable with that of Sycamore Creek, Arizona, USA (Grimm 1987), which suggests that, regardless of uncertainty associated with scaling our estimates, hyporheic N storage can be substantial in intermittent stream systems in both hot and cold climates. Importantly, we constrained our estimates of N in hyporheic OM content—by far the largest N pool—to only the top 10 cm of sediment, although the active layer thaws to depths of ≤60 cm (Conovitz et al. 2006), such that we may have underestimated the size of this pool. Ultimately, our total N storage calculations would need to be reduced by ~3 to 4 orders of magnitude to equal the highest fluxes at the stream outlet. However, such a large error is unlikely, given the number of samples and variety of sampling locations represented by the historic data that we used in our calculations. Although denitrification is possible in MDV streams (Gooseff et al. 2004b), we cannot currently estimate annual N losses from this process at the stream-corridor scale or its contribution to explaining the imbalance between import and export fluxes. Even so, it is unlikely that this process alone would exceed the multiple orders of magnitude difference between annual export masses and total storage pools, nor can it alter our finding that storage pools are many times larger than annual import fluxes. In summary, despite uncertainty related to propagating point-scale measures to the entire reach, it is highly likely that substantial N storage occurs relative to N import and export fluxes in this hyperarid, highly intermittent, polar desert stream.

Rapid reversible adsorption is an import mechanism for inorganic N storage

Physicochemical storage of NH_4^+ by adsorption to stream sediment represents a dynamic N storage process that can vary over both space and time in temperate systems while also competing with microbial N demand (Triska et al. 1994). Despite this understanding, studies of stream N budgets rarely quantify the mass of NH_4^+ adsorbed to sediment and even more rarely assess factors governing release of DIN from this pool.

Table 2. Total area-normalized N storage comparison among contrasting stream systems. Note that data appear for 2 distinct studies on Sycamore Creek, Arizona, USA. Here we present fine benthic organic matter, sensu Tank et al. (2018), as hyporheic organic matter (OM) regardless of autochthonous or allochthonous source. All values have been rounded to the nearest g/m^2 because of differences in original reporting across studies. POM = particulate organic matter.

Stream	State/ Province	Country	Latitude	Longitude	Biogeoclimatic region	N storage (g/m^2)	Dominant N storage pool	Reference
Von Guerard Stream	–	Antarctica	77.6°S	163.3°E	Antarctic	40	Hyporheic OM	This study
HJ Andrews	Oregon	USA	44.1°N	122.3°W	Temperate	12	Channel POM	Triska et al. 1984
Beaver Creek	Quebec	Canada	50.1°N	66.1°W	Subarctic	22	Channel POM	Naiman and Mellilo 1984
Sycamore Creek	Arizona	USA	33.7°N	33.7°E	Arid	3–9	Hyporheic OM	Grimm 1987
						6	Hyporheic OM	Tank et al. 2018
El Valle (PRPN)[a]	–	Panama	8.6°N	80.0°W	Tropical	4	Hyporheic OM	Tank et al. 2018
El Valle (POPN)[a]	–	Panama	8.6°N	80.0°W	Tropical	5	Hyporheic OM	Tank et al. 2018
Bear Brook	New Hampshire	USA	43.9°N	71.8°W	Temperate	10	Hyporheic OM	Tank et al. 2018
Gallina Creek	New Mexico	USA	36.6°N	105.6°W	Arid	4	Hyporheic OM	Tank et al. 2018
Santa Colona	–	Spain	41.9°N	2.6°E	Semi-arid	3	Hyporheic OM	Tank et al. 2018
Eagle Creek	Michigan	USA	42.3°N	85.3°W	Temperate	9	Hyporheic OM	Tank et al. 2018
Walker Branch	Tennessee	USA	36.0°N	84.3°W	Temperate	5	Hyporheic OM	Tank et al. 2018
Upper Ball Creek	North Carolina	USA	35.1°N	83.4°W	Temperate	2	Hyporheic OM	Tank et al. 2018
Mack Creek	Oregon	USA	44.2°N	122.2°W	Temperate	1	Hyporheic OM	Tank et al. 2018
Quebrada Bisley	–	Puerto Rico	18.3°N	65.8°W	Tropical	2	Hyporheic OM	Tank et al. 2018
Steinbogalaekur	–	Iceland	65.5°N	17.0°W	Arctic	3	Hyporheic OM	Tank et al. 2018
E1 (E1AK)[a]	Alaska	USA	68.6°N	149.6°W	Arctic	1	Hyporheic OM	Tank et al. 2018
Kings Creek	Kansas	USA	39.1°N	96.6°W	Temperate	1	Hyporheic OM	Tank et al. 2018
Lilleaa	–	Denmark	56.3°N	10.1°E	Temperate	10	Hyporheic OM	Tank et al. 2018
Kyeburn (KTNZ)[a]	–	New Zealand	45.0°S	170.4°E	Temperate	1	Hyporheic OM	Tank et al. 2018
Kyeburn (KGNZ)[a]	–	New Zealand	45.0°S	170.4°E	Temperate	1	Hyporheic OM	Tank et al. 2018

[a] Site codes used in Tank et al. (2018) are given in parentheses.

Similarly, prior studies of MDV streams have mostly ignored both the magnitude of NH_4^+ adsorption and its potential reversibility. Surprisingly, we found that the mass of N in this storage pool is about an order of magnitude larger than annual fluxes into or out of the stream corridor, suggesting that such physical storage is important in this highly oligotrophic system. Furthermore, our relatively simple laboratory assay demonstrates that NH_4^+ adsorption to MDV stream sediments is likely reversible over the range of SC observed in Von Guerard Stream over a 20+-y record. Specifically, the net release of NH_4^+ into solution increased with increasing initial SC, which represents higher initial cation concentrations (K^+ only in the assay; Fig. 5B, C). Similar sensitivity has been documented in coastal sediment at much higher SC (Seitzinger et al. 1991) but remains generally understudied in small headwater streams. The exact kinetics of NH_4^+ desorption may vary in situ, but our results indicate that 20 to 40% of adsorbed NH_4^+ can likely be released into solution rapidly (<1 h). Because adsorbed NH_4^+ content varies in space for MDV streams (Heindel et al. 2021a), channel expansion and contraction cycles with diel flow pulsing likely plays an important role in when and where such releases occur. Quantifying the net direction and magnitude of reversible NH_4^+ sorption to stream sediment on

annual timescales remains an important open question that must be answered to fully constrain the N budget of MDV streams and predict future changes.

MDV stream sediments modulate other cation fluxes (K^+, Na^+, and Li^+) through concentration-dependent adsorption and release in well-connected hyporheic zones (Gooseff et al. 2004a). This process is reflected in how specific conductivities exhibit small fluctuations during diel flow pulsing and rise during sustained low flow periods (e.g., Fig. 2A) because of evapoconcentration and hyporheic weathering (Maurice et al. 2002, Barrett et al. 2009, Singley et al. 2017). From our laboratory results, we conclude that NH_4^+ adsorption and desorption probably vary similarly over time in Von Guerard Stream. Interestingly, it is possible that the net direction of NH_4^+ adsorption may shift over time, just as occurs for other cations (Gooseff et al. 2004a). Although we cannot conclude that this behavior occurs or infer the exact conditions that may control such shifts, our findings represent an interesting topic for future investigations into how physicochemical processes govern N availability in these oligotrophic and intermittent stream corridors.

Fluxes from internal pools must sustain N availability

MDV streams have traditionally been conceptualized as net N sinks because of biological uptake by algal mats and hyporheic microbes, which can remove DIN imports over short spatial and temporal scales (e.g., Gooseff et al. 2004b, McKnight et al. 2004, Dubnick et al. 2017). Our observation that annual N imports exceeded exports for Von Guerard Stream (Fig. 4A, B) aligns well with this understanding. Additionally, stable N isotope analysis has shown a shift from a predominance of glacially sourced N in the upper reaches to autochthonously sourced N in the lower reaches of MDV streams (Kohler et al. 2018), whereas hyporheic sediment and porewater data reveal that the autochthonous POM is entrained and processed in the hyporheic zone (Heindel et al. 2021a, Singley et al. 2021b), thereby sustaining N availability along MDV streams. These findings suggest that spiraling and storage of autochthonous OM and N, rather than simply removal of allochthonous (glacially sourced) imports by biota, governs N availability along the entire reach.

Our N pool estimates indicate that there is a sufficiently large pool of N stored in the hyporheic zone to maintain DIN sourcing from the hyporheic zone even during extended periods (or whole seasons) when streamflow pulses are not large enough to mobilize POM. The same is likely true for adsorbed NH_4^+ because low flow periods result in rising SC (Fig. 2A), potentially driving releases of physically stored N (Fig. 5A) when POM import to the hyporheic zone ceases. We would expect that the relative stability of each of these N pools plays an important role in governing N availability. Diel flow pulses in MDV streams mobilize POM, especially from *Nostoc*-dominated mats, resulting in a transfer of autochthonous OM and N into the hyporheic zone (Cullis et al. 2014, Heindel et al. 2021a). Remineralization of this OM is thought to sustain elevated DIN concentrations in hyporheic water even as flow fluctuates (Singley et al. 2021b). In quantifying the extent of this hyporheic OM pool, we show that it does not need to be continually replenished to allow for DIN production by remineralization. Just as in other systems (e.g., Schmadel et al. 2021), the release of previously stored nutrients can influence (if not dominate) the fluxes observed as hydrologic conditions vary over time. Thus, this dynamic physical retention and release of OM and NH_4^+ in the hyporheic zone likely plays a critical role in sustaining N availability and downstream productivity in this highly oligotrophic system, especially at increasing distances from point allochthonous imports (i.e., the source glacier).

Implications for studies of intermittent streams in the MDVs and beyond

A few major knowledge gaps must be addressed to better constrain the longitudinal evolution of dominant N sources and actually close N budgets in MDV streams. Foremost is the need to document upstream boundary conditions for N imports, including concentration–discharge typology, DIN and DON concentrations, and meltwater hydrographs at the glacier face. Quantifying spatiotemporal variation of biological N fixation rates would further limit uncertainty surrounding N imports. There is also a need to better quantify N export dynamics for DON and POM, not just DIN. At present, none of the specific reaction rates linking these N pools (i.e., hyporheic OM mineralization, nitrification, POM entrainment, NH_4^+ adsorption/desorption, etc.) have been determined in situ. Thus, our findings raise questions about how stream corridor N pools change over time, such as: When does each pool act as a source or sink? Which pools are most sensitive to changes in streamflow, water temperature, and microbial activity that may occur with climate change? What is the importance of N in hyporheic OM pools to the recovery of periphyton following massive disturbance from large flow years (e.g., Gooseff et al. 2017)? Resolving how N pools change over time is critical for explaining how and why stream regulation of N fluxes varies over time, rather than only during narrow discrete periods (i.e., nutrient addition studies).

Beyond these questions, our study also extends the work of Salvatore et al. (2020, 2021) in demonstrating the potential to map and quantify biomass of benthic algae and the nutrients stored therein in intermittent and ephemeral streams using multispectral remote sensing imagery. For alpine, arid, and polar environments without canopy cover obscuring the streambed, this method provides a promising way to characterize spatial and temporal heterogeneity when flow is reduced or ceases altogether. A few studies have used various remote sensing platforms to map intermittent stream networks (Yang and Smith 2013, Hamada et al. 2016, Spence and Mengistu 2016). However, little

has been done to leverage such imaging to analyze exposed periphyton along the stream corridor when flow ceases, and, to our knowledge, none have attempted to quantify nutrient storage over large areas. The use of spectral libraries based on the particular system of interest offers an intriguing means to provide more nuanced characterization of biotic communities than, say, simply detecting biomass in aggregate. Applying such tools will advance investigations into the processes governing patchy and temporally variable ecosystem production, C and nutrient storage, and ecological responses to disturbance in intermittent streams.

More broadly, the results of our study taken together demonstrate that progress in the field of stream biogeochemistry may occur by more closely examining stream corridor N storage in the context of flux modulation at the reach scale, especially beyond perennial streams in forested temperate catchments. We have highlighted the utility of relatively simple scaling calculations with uncertainty propagation that serves as an initial approach for future studies in more complex systems. By applying this approach to MDV streams, we have illuminated the surprising magnitude of N storage over large regions in systems that appear starved for N.

ACKNOWLEDGEMENTS

Author contributions: JGS: conceptualization, data curation, methodology, investigation, software, formal analysis, visualization, writing (original draft, review, and editing). MRS: methodology, investigation, software, formal analysis, visualization, writing (review and editing). MNG: conceptualization, methodology, writing (review and editing). DMM: methodology, writing (review and editing). E-LSH: conceptualization, methodology, writing (review and editing).

This material is based upon work supported by the National Science Foundation Grant for Long Term Ecological Research, most recently #OPP-1637708. Funding was also provided to JGS while a graduate student by the Department of Environmental Studies and a Beverly Sears Graduate Research Grant from the University of Colorado Boulder. Any opinions, findings, conclusions, or recommendations expressed here are those of the authors and do not necessarily reflect the views of the National Science Foundation or the University of Colorado Boulder. The authors would like to acknowledge the invaluable contributions made by many field and lab team members in collecting and analyzing samples from the McMurdo Dry Valleys over the past 3 decades. All datasets used for this study are cited directly in the manuscript and are publicly available with full citation information provided below.

LITERATURE CITED

Aber, J. D., W. H. McDowell, K. J. Nadelhoffer, A. H. Magill, G. Berntson, M. Kamakea, S. G. McNulty, W. S. Currie, L. Rustad, and I. J. Fernandez. 1998. Nitrogen saturation in temperate forest ecosystems—Hypotheses revisited. Bioscience 48:921–934.

Aber, J. D., K. J. Nadelhoffer, P. Steudler, and J. M. Melillo. 1989. Nitrogen saturation in northern forest ecosystems: Excess nitrogen from fossil fuel combustion may stress the biosphere. BioScience 39:378–386.

Adams, B. J., R. D. Bardgett, E. Ayres, D. H. Wall, J. Aislabie, S. Bamforth, R. Bargagli, C. Cary, P. Cavacini, L. Connell, P. Convey, J. W. Fell, F. Frati, I. D. Hogg, K. K. Newsham, A. O'Donnell, N. Russell, R. D. Seppelt, and M. I. Stevens. 2006. Diversity and distribution of Victoria land biota. Soil Biology and Biochemistry 38:3003–3018.

Alexander, R. B., E. W. Boyer, R. A. Smith, G. E. Schwarz, and R. B. Moore. 2007. The role of headwater streams in downstream water quality. Journal of the American Water Resources Association 43:41–59.

Alger, A. S., D. M. McKnight, S. A. Spaulding, C. M. Tate, G. H. Shupe, K. A. Welch, R. Edwards, E. D. Andrews, and H. R. House. 1997. Ecological processes in a cold desert ecosystem: The abundance and species distribution of algal mats in glacial meltwater streams in Taylor Valley, Antarctica. Occasional paper 51. Institute of Arctic and Alpine Research, University of Colorado, Boulder, Colorado. (Available from: https://shorturl.at/ELUW6)

Barrett, J. E., M. N. Gooseff, and C. D. Takacs-Vesbach. 2009. Spatial variation in soil active-layer geochemistry across hydrologic margins in polar desert ecosystems. Hydrology and Earth System Sciences 13:2349–2358.

Bergstrom, A. J., and M. N. Gooseff. 2021a. Chemical and sediment characteristics of ice cores collected from the ablation zones of Canada, Commonwealth, Howard, Hughes, and Seuss Glaciers in the McMurdo Dry Valleys, Antarctica from 2015 to 2019. Environmental Data Initiative, Madison, Wisconsin. (Available from: https://mcm.lternet.edu/content/chemical-and-sediment-characteristics-ice-cores-collected-ablation-zones-canada-commonwealth, Accessed 3 June 2021)

Bergstrom, A. J., and M. N. Gooseff. 2021b. Chemical characteristics of supraglacial stream water on Canada Glacier, McMurdo Dry Valleys, Antarctica during the 2015–2016 austral summer. Environmental Data Initiative, Madison, Wisconsin. (Available from: https://mcm.lternet.edu/content/chemical-characteristics-supraglacial-stream-water-canada-glacier-mcmurdo-dry-valleys, Accessed 3 June 2021)

Bergstrom, A. J., M. N. Gooseff, J. G. Singley, M. J. Cohen, and K. A. Welch. 2020. Nutrient uptake in the supraglacial stream network of an Antarctic glacier. Journal of Geophysical Research: Biogeosciences 125:e2020JG005679.

Bernhardt, E. S., G. E. Likens, R. O. Hall, D. C. Buso, S. G. Fisher, T. M. Burton, J. L. Meyer, W. H. McDowell, M. S. Mayer, and W. B. Bowden. 2005. Can't see the forest for the stream? In-stream processing and terrestrial nitrogen exports. BioScience 55:219–230.

Bockheim, J. G., I. B. Campbell, and M. McLeod. 2007. Permafrost distribution and active-layer depths in the McMurdo Dry valleys, Antarctica. Permafrost and Periglacial Processes 18:217–227.

Borchers, H. W. 2021. *pracma*: Practical numerical math functions. (Available from: https://cran.r-project.org/web/packages/pracma/index.html)

Boyer, E. W., C. L. Goodale, N. A. Jaworski, and R. W. Howarth. 2002. Anthropogenic nitrogen sources and relationships to riverine nitrogen export in the northeastern USA. Biogeochemistry 57:137–169.

Burns, D. A. 1998. Retention of NO_3^- in an upland streamenvironment: A mass balance approach. Biogeochemistry 40:73–96.

Burrows, R. M., H. Rutlidge, N. R. Bond, S. M. Eberhard, A. Auhl, M. S. Andersen, D. G. Valdez, and M. J. Kennard. 2017. High rates of organic carbon processing in the hyporheic zone of intermittent streams. Scientific Reports 7:13198.

Conovitz, P. A., L. H. MacDonald, and D. M. McKnight. 2006. Spatial and temporal active layer dynamics along three glacial meltwater streams in the McMurdo Dry Valleys, Antarctica. Arctic, Antarctic, and Alpine Research 38:42–53.

Cullis, J. D. S., L. F. Stanish, and D. M. McKnight. 2014. Diel flow pulses drive particulate organic matter transport from microbial mats in a glacial meltwater stream in the McMurdo Dry Valleys. Water Resources Research 50:86–97.

Datry, T., N. Bonada, and A. J. Boulton. 2017. Intermittent rivers and ephemeral streams: Ecology and management. Academic Press, San Diego, California.

Delignette-Muller, M. L., and C. Dutang. 2015. *fitdistrplus*: An R package for fitting distributions. Journal of Statistical Software 64:1–34.

Deuerling, K. M., W. B. Lyons, S. A. Welch, and K. A. Welch. 2014. The characterization and role of aeolian deposition on water quality, McMurdo Dry Valleys, Antarctica. Aeolian Research 13:7–17.

Dodds, W. K., V. H. Smith, and K. Lohman. 2002. Nitrogen and phosphorus relationships to benthic algal biomass in temperate streams. Canadian Journal of Fisheries and Aquatic Sciences 59:865–874.

Doran, P. T., C. P. McKay, G. D. Clow, G. L. Dana, A. G. Fountain, T. Nylen, and W. B. Lyons. 2002. Valley floor climate observations from the McMurdo Dry Valleys, Antarctica, 1986–2000. Journal of Geophysical Research: Atmospheres 107:ACL13-1–ACL13-12.

Drummond, J. D., S. Bernal, D. von Schiller, and E. Martí. 2016. Linking in-stream nutrient uptake to hydrologic retention in two headwater streams. Freshwater Science 35:1176–1188.

Dubnick, A., J. Wadham, M. Tranter, M. Sharp, J. Orwin, J. Barker, E. Bagshaw, and S. Fitzsimons. 2017. Trickle or treat: The dynamics of nutrient export from polar glaciers. Hydrological Processes 31:1776–1789.

Duncan, J. M., L. E. Band, P. M. Groffman, and E. S. Bernhardt. 2015. Mechanisms driving the seasonality of catchment scale nitrate export: Evidence for riparian ecohydrologic controls. Water Resources Research 51:3982–3997.

Fountain, A. G., T. Nylen, A. Monaghan, H. J. Basagic, and D. Bromwich. 2010. Snow in the McMurdo dry valleys, Antarctica. International Journal of Climatology 30:633–642.

Gómez, R., V. García, M. R. Vidal-Abarca, and L. Suárez. 2009. Effect of intermittency on N spatial variability in an arid Mediterranean stream. Journal of the North American Benthological Society 28:572–583.

Gomez-Velez, J. D., J. W. Harvey, M. Bayani Cardenas, and B. Kiel. 2015. Denitrification in the Mississippi River network controlled by flow through river bedforms. Nature Geoscience 8:941.

Gooseff, M. N., J. E. Barrett, B. J. Adams, P. T. Doran, A. G. Fountain, W. B. Lyons, D. M. McKnight, J. C. Priscu, E. R. Sokol, C. Takacs-Vesbach, M. L. Vandegehuchte, R. A. Virginia, and D. H. Wall. 2017. Decadal ecosystem response to an anomalous melt season in a polar desert in Antarctica. Nature Ecology & Evolution 1:1334–1338.

Gooseff, M. N., and W. B. Lyons. 2022. Nitrogen and phosphorus concentrations in glacial meltwater streams, McMurdo Dry Valleys, Antarctica (1993–2020, ongoing). Version 7. Environmental Data Initiative, Madison, Wisconsin. (Available from: https://portal.edirepository.org/nis/mapbrowse?packageid=knb-lter-mcm.21.7, Accessed February 2021)

Gooseff, M. N., and D. M. McKnight. 2019. Seasonal high-frequency measurements of discharge, water temperature, and specific conductivity from Von Guerard Stream at F6, McMurdo Dry Valleys, Antarctica (1990–2019, ongoing). Version 18. Environmental Data Initiative, Madison, Wisconsin. (Available from: https://portal.edirepository.org/nis/mapbrowse?packageid=knb-lter-mcm.9027.19, Accessed February 2021)

Gooseff, M. N., D. M. McKnight, P. T. Doran, A. G. Fountain, and W. B. Lyons. 2011. Hydrological connectivity of the landscape of the McMurdo Dry Valleys, Antarctica. Geography Compass 5:666–681.

Gooseff, M. N., D. M. McKnight, and R. L. Runkel. 2004a. Reach-scale cation exchange controls on major ion chemistry of an Antarctic glacial meltwater stream. Aquatic Geochemistry 10:221–238.

Gooseff, M. N., D. M. McKnight, R. L. Runkel, and J. H. Duff. 2004b. Denitrification and hydrologic transient storage in a glacial meltwater stream, McMurdo Dry Valleys, Antarctica. Limnology and Oceanography 49:1884–1895.

Gooseff, M. N., A. N. Wlostowski, D. M. McKnight, and C. Jaros. 2016. Hydrologic connectivity and implications for ecosystem processes–Lessons from naked watersheds. Geomorphology 277:63–71.

Grimm, N. B. 1987. Nitrogen dynamics during succession in a desert stream. Ecology 68:1157–1170.

Hamada, Y., B. L. O'Connor, A. B. Orr, and K. K. Wuthrich. 2016. Mapping ephemeral stream networks in desert environments using very-high-spatial-resolution multispectral remote sensing. Journal of Arid Environments 130:40–48.

Harvey, J. W., J. D. Gomez-Velez, N. M. Schmadel, D. T. Scott, E. W. Boyer, R. B. Alexander, K. Eng, H. Golden, A. Kettner, C. Konrad, R. B. Moore, J. Pizzuto, G. E. Schwarz, C. Soulsby, and J. Choi. 2018. How hydrologic connectivity regulates water quality in river corridors. Journal of the American Water Resources Association 55:369–381.

Heindel, R. C., A. J. Bergstrom, J. G. Singley, D. M. McKnight, J. Darling, B. Lukkari, K. A. Welch, and M. N. Gooseff. 2021a. Diatoms in hyporheic sediments trace organic matter retention and processing in the McMurdo Dry Valleys, Antarctica. Journal of Geophysical Research: Biogeosciences 126:JG006097.

Heindel, R. C., J. G. Singley, A. J. Bergstrom, J. Darling, K. A. Welch, D. M. McKnight, and M. N. Gooseff. 2021b. Hyporheic sediment characteristics from Von Guerard Stream, Taylor Valley, McMurdo Dry Valleys, Antarctica in January 2019. Version 2. Environmental Data Initiative, Madison, Wisconsin. (Available from: https://mcm.lternet.edu/content/hyporheic-sediment-characteristics-von-guerard-stream-taylor-valley-mcmurdo-dry-valleys, Accessed February 2021)

Hillebrand, H. 2008. Grazing regulates the spatial variability of periphyton biomass. Ecology 89:165–173.

Horner, R. R., and E. B. Welch. 1981. Stream periphyton development in relation to current velocity and nutrients. Canadian Journal of Fisheries and Aquatic Sciences 38:449–457.

Howard-Williams, C., J. C. Priscu, and W. F. Vincent. 1989. Nitrogen dynamics in two antarctic streams. Hydrobiologia 172:51–61.

Koch, J. C., D. M. McKnight, and J. L. Baeseman. 2010. Effect of unsteady flow on nitrate loss in an oligotrophic, glacial meltwater stream. Journal of Geophysical Research: Biogeosciences 115:G01001.

Koch, R., D. Kerling, and J. M. O'Brien. 2018. Effects of chronic elevated nitrate concentrations on the structure and function of river biofilms. Freshwater Biology 63:1199–1210.

Kohler, T. J. 2018. McMurdo Dry Valleys microbial mat biomass, isotopes, and nutrient ratios sampled over a longitudinal gradient of two McMurdo Dry Valley streams. Version 2. Environmental Data Initiative, Madison, Wisconsin. (Available from: https://portal.edirepository.org/nis/mapbrowse?scope=knb-lter-mcm&identifier=9031, Accessed February 2021)

Kohler, T. J., L. F. Stanish, S. W. Crisp, J. C. Koch, D. Liptzin, J. L. Baeseman, and D. M. McKnight. 2015. Life in the main channel: Long-term hydrologic control of microbial mat abundance in McMurdo Dry Valley streams, Antarctica. Ecosystems 18:310–327.

Kohler, T. J., L. F. Stanish, D. Liptzin, J. E. Barrett, and D. M. McKnight. 2018. Catch and release: Hyporheic retention and mineralization of N-fixing *Nostoc* sustains downstream microbial mat biomass in two polar desert streams. Limnology and Oceanography Letters 3:357–364.

Lovett, G. M., and C. L. Goodale. 2011. A new conceptual model of nitrogen saturation based on experimental nitrogen addition to an oak forest. Ecosystems 14:615–631.

Luce, J. J., A. Cattaneo, and M. F. Lapointe. 2010. Spatial patterns in periphyton biomass after low-magnitude flow spates: Geomorphic factors affecting patchiness across gravel–cobble riffles. Journal of the North American Benthological Society 29:614–626.

Maurice, P. A., D. M. McKnight, L. Leff, J. E. Fulghum, and M. N. Gooseff. 2002. Direct observations of aluminosilicate weathering in the hyporheic zone of an Antarctic Dry Valley stream. Geochimica et Cosmochimica Acta 66:1335–1347.

McKnight, D. M. 2019. Algal microbial mat biomass measurements from the McMurdo Dry Valleys and Cape Royds, Antarctica (1994–2019, ongoing). Environmental Data Initiative, Madison, Wisconsin. (Available from: https://mcm.lternet.edu/content/algal-microbial-mat-biomass-measurements-mcmurdo-dry-valleys-and-cape-royds-antarctica-1994, Accessed February 2020)

McKnight, D. M., A. Alger, C. Tate, G. Shupe, and S. Spaulding. 1998. Longitudinal patterns in algal abundance and species distribution in meltwater streams in Taylor Valley, Southern Victoria Land, Antarctica. Pages 109–127 *in* J. C. Priscu (editor). Ecosystem dynamics in a polar desert: The McMurdo Dry Valleys, Antarctica. American Geophysical Union 72.

McKnight, D. M., K. D. Cozzetto, J. D. S. Cullis, M. N. Gooseff, C. Jaros, J. C. Koch, W. B. Lyons, R. Neupauer, and A. N. Wlostowski. 2015. Potential for real-time understanding of coupled hydrologic and biogeochemical processes in stream ecosystems: Future integration of telemetered data with process models for glacial meltwater streams. Water Resources Research 51:6725–6738.

McKnight, D. M., D. K. Niyogi, A. S. Alger, A. Bomblies, P. A. Conovitz, and C. M. Tate. 1999. Dry valley streams in Antarctica: Ecosystems waiting for water. BioScience 49:985–995.

McKnight, D. M., R. L. Runkel, C. M. Tate, J. H. Duff, and D. L. Moorhead. 2004. Inorganic N and P dynamics of Antarctic glacial meltwater streams as controlled by hyporheic exchange and benthic autotrophic communities. Journal of the North American Benthological Society 23:171–188.

McKnight, D. M., C. M. Tate, E. Andrews, D. Niyogi, K. D. Cozzetto, K. Welch, W. B. Lyons, and D. Capone. 2007. Reactivation of a cryptobiotic stream ecosystem in the McMurdo Dry Valleys, Antarctica: A long-term geomorphological experiment. Geomorphology 89:186–204.

Mikucki, J., E. Auken, S. Tulaczyk, R. A. Virginia, C. Schamper, K. I. Sørensen, P. T. Doran, H. Dugan, and N. Foley. 2015. Deep groundwater and potential subsurface habitats beneath an Antarctic dry valley. Nature Communications 6:6831.

Naiman, R. J., and J. M. Melillo. 1984. Nitrogen budget of a subarctic stream altered by beaver (*Castor canadensis*). Oecologia 62:150–155.

O'Brien, J. M., S. K. Hamilton, L. Podzikowski, and N. Ostrom. 2012. The fate of assimilated nitrogen in streams: An in situ benthic chamber study. Freshwater Biology 57:1113–1125.

Peterson, B. J., W. M. Wollheim, P. J. Mulholland, J. R. Webster, J. L. Meyer, J. L. Tank, E. Martí, W. B. Bowden, H. M. Valett, and A. E. Hershey. 2001. Control of nitrogen export from watersheds by headwater streams. Science 292:86–90.

Salvatore, M. R., J. E. Barrett, S. R. Borges, S. N. Power, L. F. Stanish, E. R. Sokol, and M. N. Gooseff. 2021. Counting carbon: Quantifying biomass in the McMurdo Dry Valleys through orbital & field observations. International Journal of Remote Sensing 42:8597–8623.

Salvatore, M. R., S. R. Borges, J. E. Barrett, E. R. Sokol, L. F. Stanish, S. N. Power, and P. Morin. 2020. Remote characterization of photosynthetic communities in the Fryxell basin of Taylor Valley, Antarctica. Antarctic Science 32:255–270.

Schmadel, N. M., J. W. Harvey, and G. E. Schwarz. 2021. Seasonally dynamic nutrient modeling quantifies storage lags and time-varying reactivity across large river basins. Environmental Research Letters 16:095004.

Seitzinger, S., J. A. Harrison, J. K. Böhlke, A. F. Bouwman, R. Lowrance, B. Peterson, C. Tobias, and G. Van Drecht. 2006. Denitrification across landscapes and waterscapes: A synthesis. Ecological Applications 16:2064–2090.

Seitzinger, S. P., W. S. Gardner, and A. K. Spratt. 1991. The effect of salinity on ammonium sorption in aquatic sediments: Implications for benthic nutrient recycling. Estuaries 14:167–174.

Shumilova, O., D. Zak, T. Datry, D. Schiller, R. Corti, A. Foulquier, B. Obrador, K. Tockner, D. C. Allan, F. Altermatt, M. I. Arce, S. Arnon, D. Banas, A. Banegas-Medina, E. Beller, M. L. Blanchette, J. F. Blanco-Libreros, J. Blessing, I. Gonçalves Boëchat, K. Boersma, M. T. Bogan, N. Bonada, N. R. Bond, K. Brintrup, A. Bruder, R. Burrows, T. Cancellario, S. M. Carlson, S. Cauvy-Fraunié, N. Cid, M. Danger, B. de Freitas Terra, A. M. De Girolamo, Ruben del Campo, F. Dyer, A. Elosegi, E. Faye, C. Febria, R. Figueroa, B. Four, M. O. Gessner, P. Gnohossou, R. Gómez Cerezo, L. Gomez-Gener, M. A.S. Graça, S. Guareschi, B. Gücker, J. L. Hwan, S. Kubheka, S. D. Langhans, C. Leigh, C. J. Little, S. Lorenz, J. Marshall, A. McIntosh, C. Mendoza-Lera, E. Irmgard Meyer, M. Miliša, M. C. Mlambo, M. Moleón, P. Negus, D. Niyogi, A. Papatheodoulou, I. Pardo, P. Paril, V. Pešić, P. Rodriguez-Lozano, R. J. Rolls, M. M.

Sanchez-Montoya, A. Savić, A. Steward, R. Stubbington, A. Taleb, R. Vander Vorste, N. Waltham, A. Zoppini, and C. Zarfl. 2019. Simulating rewetting events in intermittent rivers and ephemeral streams: A global analysis of leached nutrients and organic matter. Global Change Biology 25:1591–1611.

Singley, J. G., M. N. Gooseff, D. M. McKnight, and E.-L. S. Hinckley. 2021a. Surface and hyporheic porewater chemistry and sediment nitrification potentials in Von Guerard Stream, McMurdo Dry Valleys, Antarctica (2018–2020). Version 2. Environmental Data Initiative, Madison, Wisconsin. (Available from: https://mcm.lternet.edu/content/surface-and-hyporheic-porewater-chemistry-and-sediment-nitrification-potentials-von-guerard, Accessed March 2021)

Singley, J. G., M. N. Gooseff, D. M. McKnight, and E.-L. S. Hinckley. 2021b. The role of hyporheic connectivity in determining nitrogen availability: Insights from an intermittent Antarctic stream. Journal of Geophysical Research: Biogeosciences 126:JG006309.

Singley, J. G., A. N. Wlostowski, A. J. Bergstrom, E. R. Sokol, C. L. Torrens, C. Jaros, C. E. Wilson, P. J. Hendrickson, and M. N. Gooseff. 2017. Characterizing hyporheic exchange processes using high-frequency electrical conductivity-discharge relationships on subhourly to interannual timescales. Water Resources Research 53:4124–4141.

Spence, C., and S. Mengistu. 2016. Deployment of an unmanned aerial system to assist in mapping an intermittent stream. Hydrological Processes 30:493–500.

SMC APHA (Standard Methods Committee of the American Public Health Association), American Water Works Association, and Water Environment Federation. 2018a. 4500-NH_3 nitrogen (ammonia). *In* W. C. Lipps, T. E. Baxter, and E. Braun-Howland (editors). APHA Press: Washington, DC. Available from: https://www.standardmethods.org/doi/10.2105/SMWW.2882.087, Accessed January 2021)

SMC APHA (Standard Methods Committee of the American Public Health Association), American Water Works Association, and Water Environment Federation. 2018b. 4500-NO_3^- nitrogen (nitrate). *In* W. C. Lipps, T. E. Baxter, and E. Braun-Howland (editors). APHA Press: Washington, DC. (Available from: https://www.standardmethods.org/doi/abs/10.2105/SMWW.2882.089, Accessed January 2021)

Stelzer, R. S., and G. A. Lamberti. 2001. Effects of N:P ratio and total nutrient concentration on stream periphyton community structure, biomass, and elemental composition. Limnology and Oceanography 46:356–367.

Tank, J. L., E. Martí, T. Riis, D. von Schiller, A. J. Reisinger, W. K. Dodds, M. R. Whiles, L. R. Ashkenas, W. B. Bowden, S. M. Collins, C. L. Crenshaw, T. A. Crowl, N. A. Griffiths, N. B. Grimm, S. K. Hamilton, S. L. Johnson, W. H. McDowell, B. M. Norman, E. J. Rosi, K. S. Simon, S. A. Thomas, and J. R. Webster. 2018. Partitioning assimilatory nitrogen uptake in streams: An analysis of stable isotope tracer additions across continents. Ecological Monographs 88:120–138.

Triska, F. J., A. P. Jackman, J. H. Duff, and R. J. Avanzino. 1994. Ammonium sorption to channel and riparian sediments: A transient storage pool for dissolved inorganic nitrogen. Biogeochemistry 26:67–83.

Triska, F. J., J. R. Sedell, K. Cromack, S. V. Gregory, and F. M. McCorison. 1984. Nitrogen budget for a small coniferous forest stream. Ecological Monographs 54:119–140.

Vitousek, P. M., and W. A. Reiners. 1975. Ecosystem succession and nutrient retention: A hypothesis. BioScience 25:376–381.

von Schiller, D., E. Martí, J. L. Riera, and F. Sabater. 2007. Effects of nutrients and light on periphyton biomass and nitrogen uptake in Mediterranean streams with contrasting land uses. Freshwater Biology 52:891–906.

Witherow, R. A., W. B. Lyons, N. A. N. Bertler, K. A. Welch, P. A. Mayewski, S. B. Sneed, T. Nylen, M. J. Handley, and A. Fountain. 2006. The aeolian flux of calcium, chloride and nitrate to the McMurdo Dry Valleys landscape: Evidence from snow pit analysis. Antarctic Science 18:497–505.

Wlostowski, A. N., M. N. Gooseff, D. M. McKnight, C. Jaros, and W. B. Lyons. 2016. Patterns of hydrologic connectivity in the McMurdo Dry Valleys, Antarctica: A synthesis of 20 years of hydrologic data. Hydrological Processes 30:2958–2975.

Yang, K., and L. C. Smith. 2013. Supraglacial streams on the greenland ice sheet delineated from combined spectral-shape information in high-resolution satellite imagery. Institute of Electrical and Electronics Engineers: Geoscience and Remote Sensing Letters 10:801–805.